AFRL-AFOSR-UK-TR-2015-0007

High-mobility two-dimensional electron gases at ZnO/ZnMgO interfaces for ultra-fast electronics applications

Prof. Paul Warburton

UNIVERSITY COLLEGE LONDON
GOWER STREET
LONDON, WC1E 6BT
UNITED KINGDOM

EOARD GRANT #FA8655-12-1-2126

Report Date: November 2014

Final Report from 1 August 2012 to 30 July 2014

Air Force Research Laboratory
Air Force Office of Scientific Research
European Office of Aerospace Research and Development
Unit 4515, APO AE 09421-4515

REPORT DOCUMENTATION PAGE

Form Approved OMB No. 0704-0188

1. REPORT DATE *(DD-MM-YYYY)*	2. REPORT TYPE	3. DATES COVERED *(From – To)*
17 November 2014	Final Report	1 August 2012 –30 July 2014

4. TITLE AND SUBTITLE

High-mobility two-dimensional electron gases at ZnO/ZnMgO interfaces for ultra-fast electronics applications

5a. CONTRACT NUMBER

5b. GRANT NUMBER

FA8655-12-1-2126

5c. PROGRAM ELEMENT NUMBER

61102F

6. AUTHOR(S)

Prof. Paul Warburton

5d. PROJECT NUMBER

5d. TASK NUMBER

5e. WORK UNIT NUMBER

7. PERFORMING ORGANIZATION NAME(S) AND ADDRESS(ES)

UNIVERSITY COLLEGE LONDON
GOWER STREET
LONDON, WC1E 6BT

8. PERFORMING ORGANIZATION REPORT NUMBER

N/A

9. SPONSORING/MONITORING AGENCY NAME(S) AND ADDRESS(ES)

EOARD
Unit 4515
APO AE 09421-4515

10. SPONSOR/MONITOR'S ACRONYM(S)

AFRL/AFOSR/IOE (EOARD)

11. SPONSOR/MONITOR'S REPORT NUMBER(S)

AFRL-AFOSR-UK-TR-2015-0007

12. DISTRIBUTION/AVAILABILITY STATEMENT

Distribution A: Approved for public release; distribution is unlimited.

13. SUPPLEMENTARY NOTES

14. ABSTRACT

We have measured high mobility electron transport at the interface between insulating zinc oxide and zinc magnesium oxide films grown by molecular beam epitaxy. A maximum electron mobility exceeding 2200 cm2V-1s-1 was measured. Spectroscopic depth-profiling of the films shows however that these high mobilities can only be obtained in films where the spatial variation of the magnesium content does not show a sharp discontinuity at the interface. This suggests that higher mobilities can be obtained in the future by controlling the competing effects of interface strain and electron confinement. Ongoing work therefore will focus on tailoring the properties of the interface during growth so as to simultaneously maximise the electron confinement and minimise the strain. This will necessitate the growth of a thin film of ZnO between the ZnO single crystal substrate and the ZnMgO thin film.

15. SUBJECT TERMS

EOARD, compound III-V and oxide semiconductors, London Centre for Nanotechnology, nanoscale field-effect transistors, spintronics, THz sources and electronics, ZnO superlattices, ZnO/ZnMgO heterostructures

16. SECURITY CLASSIFICATION OF:			17. LIMITATION OF ABSTRACT	18, NUMBER OF PAGES	19a. NAME OF RESPONSIBLE PERSON
a. REPORT	b. ABSTRACT	c. THIS PAGE			John Gonglewski
UNCLAS	UNCLAS	UNCLAS	SAR	13	19b. TELEPHONE NUMBER *(Include area code)* +44 (0)1895 616007

Final Report

Grant Number: **FA8655-12-1-2126**

Research Title: **High-mobility two-dimensional electron gases at ZnO/ZnMgO interfaces for ultra-fast electronics applications**

PI Name: **Prof. Paul Warburton, University College London**

Period of Performance: 1st August 2012 to 30th July 2014

Table of Contents

List of Figures

Summary

We have measured high mobility electron transport at the interface between insulating zinc oxide and zinc magnesium oxide films grown by molecular beam epitaxy. A maximum electron mobility exceeding 2200 $cm^2V^{-1}s^{-1}$ was measured. Spectroscopic depth-profiling of the films shows however that these high mobilities can only be obtained in films where the spatial variation of the magnesium content does not show a sharp discontinuity at the interface. This suggests that higher mobilities can be obtained in the future by controlling the competing effects of interface strain and electron confinement.

1 Introduction

Future high-speed electronic and spintronic devices will rely upon materials with new functional tuneable properties. Correlated-electron oxide materials have been widely studied since their functional properties can be tuned by doping – for example between magnetic and superconducting states. For such materials to make an impact in the context of DOD missions, it will be necessary for the electrons to have very high mobility, thereby maximizing the switching speed of the devices. ZnO/ZnMgO heterostructures show very high mobility, approaching values obtained with GaAs. The combination of the tuneable functionality inherent to oxides and the high mobility suggest emerging technology paradigms for application in high-density low-power ferroelectric memory devices (FRAM), low-power spintronic devices switched by voltage rather than current and THz sources based on ZnO/ZnMgO superlattices.

Two strands of research have dominated the experimental solid-state electronic device physics agenda in the last twenty years or so: (i) the study of strongly-correlated electron systems in oxides, enabling materials whose functionality (e.g. ferromagnetism, superconductivity, ferroelectricity, multiferroicity) can be tuned by doping; (ii) the study of electronic systems in reduced dimensions – including two-dimensional electron gases and quantum dots in compound semiconductors such as GaAs. In this project we unite these strands, using the quantum confinement at the ZnO/ZnMgO interface to study the effect of reduced dimensionality on the strongly-correlated electrons in the ferroelectric material zinc oxide. The ZnO / ZnMgO system is far less-widely studied than the $LaAlO_3/SrTiO_3$ system.

In our work we have developed molecular-beam epitaxy techniques for growing ZnMgO films on single crystal ZnO substrates. By controlling the growth conditions (specifically the Mg and O fluxes and the growth temperature) we have been able to grow two types of ZnMgO films: Type I, in which the Mg concentration in the film is approximately constant, with a sharp discontinuity of the Mg concentration at the interface with the substrate; and Type II, in which the Mg concentration increases monotonically from the interface with the substrate to the top surface of the film. The discontinuity in the Type I films should in principle lead to stronger two-dimensional electron confinement and hence higher mobility. We experimentally find, however, that Type II films display higher electron mobility than Type I films. This is caused by strain at the interface resulting from the discontinuous change of lattice constant in Type I films. The relaxation of this strain caused by redistribution of the Mg atoms during MBE growth in Type II films results in higher mobilities in spite of the reduced electron confinement.

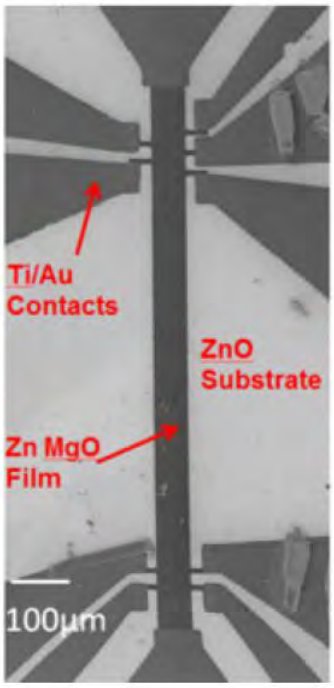

Figure 1 : He-ion microscope image of a fabricated ZnMgO device with multiple Ti/Au wiring contacts for longitudinal and transverse electrical measurements.

Ongoing work will focus on growth of ZnO-ZnMgO thin film *bilayers* on ZnO substrates. This will give us increased control over the interface properties, potentially allowing us to simultaneously maximise electron confinement while minimising interface strain.

2 Methods, Assumptions, Procedures

2.1 Film Growth by Molecular-Beam Epitaxy

ZnMgO thin films were grown on [0001] single crystal substrates. The substrates were backed with 300nm of titanium to absorb heat from the MBE radiative heater. Zn and Mg fluxes were measured by a retractable ion flux gauge. Substrates were heated to the specified temperature over 20 mins under vacuum with a large degassing occurring at 400°C. The oxygen plasma is ignited at 600°C with all shutters closed. Once the growth temperature is stabilised (as determined by pyrometry) all shutters were opened and growth started. The substrate was rotated at 20 rpm. During growth the films are analysed in situ using reflection high-energy electron diffraction (RHEED) with a 20 keV electron-beam. The growth time is one hour, with the sample being cooled under vacuum once all shutters were closed and the oxygen plasma switched off.

2.2 Film Characterisation

Films were routinely characterised by x-ray diffraction, x-ray photoemission spectroscopy, atomic force microscopy, scanning electron microscopy and scanning helium-ion microscopy.

2.3 Device Fabrication and Measurement

Films were fabricated into multi-terminal structures to characterise the longitudinal and transverse resistivities. The samples are cleaned in acetone/IPA/water and then dehydrated for 30 mins at 200 °C. Optical lithography is used to define the device geometry. A mesa is argon milled to a depth of 200 nm. The mesa is contacted via a sputtered Ti (8 nm)/Au (50 nm) bilayer. This is followed by sputtering of aluminium oxide as a dielectric barrier before finally the gate electrode was sputtered Ti (8 nm)/ Au (50 nm). A fabricated device is shown in figure 1 (this particular device has no gate electrode).

Four terminal current-source electrical transport measurements were performed using a Quantum Design PPMS system with a ^{3}He insert. The base temperature is 400 mK and a field of up to 14 T can be applied perpendicular to the ZnO/ZnMgO interface.

3 Results and Discussion

3.1 Introduction

Selection of the appropriate substrate is vital in determining the ZnMgO-ZnO interface quality. Due to the polarity of ZnO, growth on different faces results in widely differing functional properties. Both the [0001] and [000-1] surfaces are favoured due to their being polar and energetically stable compared to other faces. Of these two the oxygen-polar [000-1] face is smoother but with a smaller electron accumulation layer and a smaller magnitude of band bending, V_{bb}. This surface therefore does not meet the conditions necessary for the strong polarization effects needed for the formation of a 2DEG. We therefore focus on the zinc-polar [0001] face, which has a higher value of V_{bb}. At the ZnO/ZnMgO interface the surface charge is left uncompensated due to the difference in polarization. This subsequently leads to the large internal electric field for confinement of the 2DEG.

Due to the surface heavily dictating the morphology of the subsequent films it is important that the treatment of the substrates before growth creates an atomically smooth film. The substrates as received are hydrothermally grown and polished with a maximum 0.5° off cut. Heating the substrate up to 800°C under vacuum showed no significant change in surface morphology when observed via RHEED and AFM. Under an oxygen flow the surface degenerates when heated. However, a better surface morphology was obtained for temperatures above 1400°C. Currently films are grown directly onto as-received substrates which have only been subject to a typical solvent cleaning procedure (sonication in acetone then IPA then deionized water followed by 20 minute dehydration at 200°C under atmosphere).

There is a compromise between the growth rate and the roughness of the film when determining the optimum conditions. If the deposition rate is low, the impurity incorporation will be much higher. These films are observed to be much smoother than those grown at a higher deposition rate. If the film rate is high then there will be a larger concentration of dislocations and grain boundaries causing a larger degree of roughness, but the impurity concentration will be much lower. The flux of Zn (and/or Mg) and oxygen in the molecular beam determines both the number of atoms available at the surface for film nucleation and growth. The metal:oxygen ratio can be controlled via the oxygen plasma flow and the zinc and magnesium flux to create metallic or oxygen rich environments for the film to grow in.

With the difference between the crystal structures of MgO (rock salt) and ZnO (wurtzite), the formation of ZnMgO requires a metastable state. The solubility limit of Mg in ZnO in bulk is 4%. However, solubilities as high as 49% have been achieved for thin films with no MgO segregation [1]. The incorporation of the Mg into the film has to be optimized due to its effects on two competing electron transport processes at the interface. If the Mg content is too high, the lattice mismatch at the interface results in interface roughness scattering. This then becomes a limiting mechanism to the mobility at the interface [2]. With low Mg content the band offset is reduced leading to reduced carrier confinement at the interface.

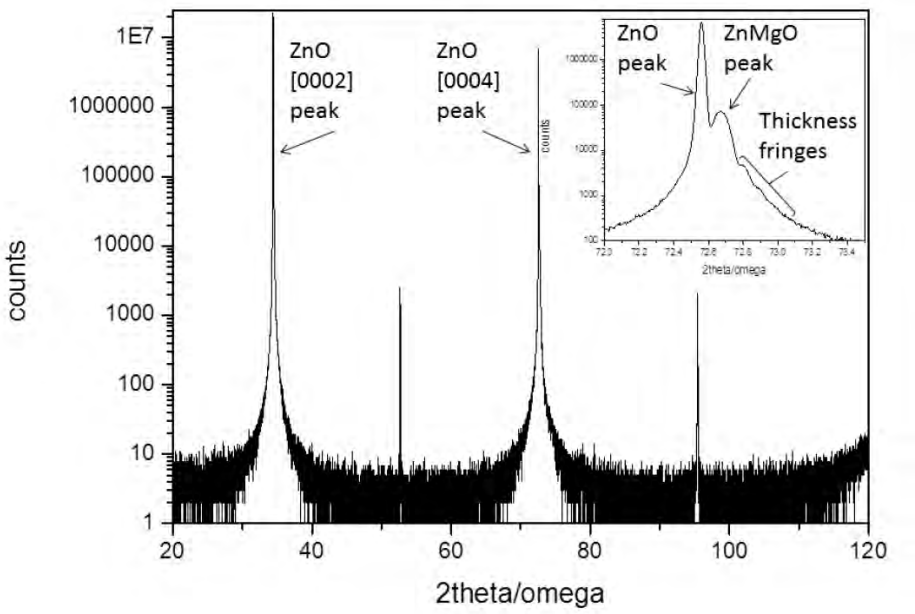

Figure 2: X-ray diffraction scan for a Type I ZnMgO film. The scan is dominated by substrate peaks. A magnified view of the [0004] peak (inset) shows (a) a smaller peak from the ZnMgO film and (b) interference fringes caused by multiple reflections at the ZnMgO-ZnO interface.

3.2 Determination of Optimum Growth Conditions

3.2.1 Mg Incorporation

It has previously been shown that a slightly oxygen rich environment is favoured for Zn-polar ZnO [3], so as a starting point the Zn beam flux was set at $4x10^{-7}$ Torr, the oxygen flux at 3sccm, and the substrate heated to 750 °C. The Zn and oxygen flux were kept constant and the Mg flux was varied between 2.5% and 25% of the Zn flux. The films varied greatly in morphology and composition. Figure 2 shows a typical x-ray diffraction θ - 2θ scan for a ZnMgO film. The scan is dominated by the diffraction peaks from the crystalline ZnO substrate. The inset however clearly shows both the ZnMgO diffraction peak and fringes resulting from finite thickness of the ZnMgO film. From the position of the ZnMgO diffraction peak one can extract the Mg content of the film as shown in figure 3.

XRD analysis showed that those films with a Mg:Zn flux ratio exceeding 11% displayed segregation into separate ZnMgO and MgO phases This can be seen as a discontinuity in the Mg content as shown

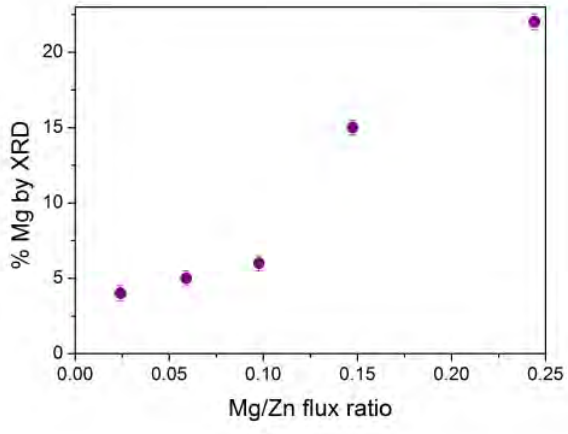

Figure 3: Mg incorporation determined by XRD with varying Zn:Mg ratio with a constant oxygen plasma flow of 3 sccm and a constant Zn flux 4 x 10^{-7} Torr

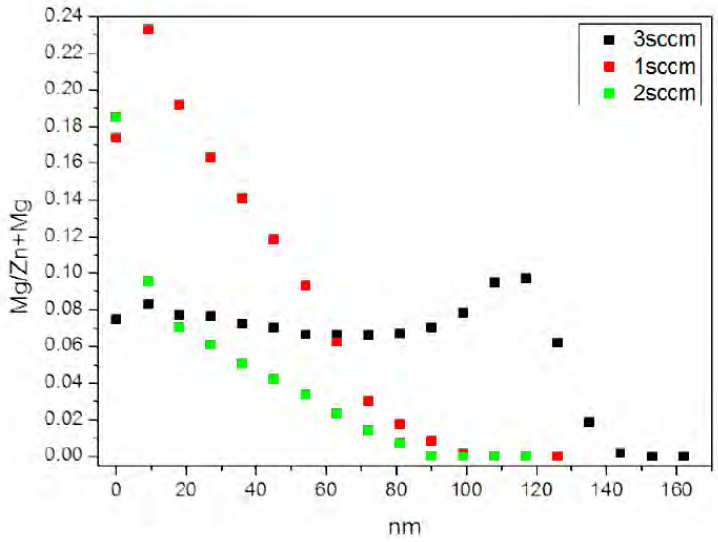

Figure 4: Fractional Mg content in ZnMgO as function of distance from the top surface of the film obtained using XPS depth profiling. The films are nominally 100 to 120 nm thick. The film grown with 3 sccm oxygen flow (black) is Type I, with approximately constant Mg concentration throughout the film. The films grown at 1 (red) and 2 (green) sccm oxygen flow are Type II with an approximately linear depth profile of Mg.

in figure 3. Due to this segregation only films below this 11% of Mg:Zn flux ratio threshold are considered.

3.2.2 Varying Oxygen Flow

Having established that a Mg/Zn flux ratio of 0.1 worked well in creating a homogeneous film with an abrupt interface, the oxygen flux was reduced from 3 sccm to 1 sccm. The result was a film that no longer showed a homogeneous concentration of Mg through the film but instead showed an approximately linear decrease of Mg content through the film thickness. This was observed by XPS depth profiling as shown in figure 4.

With a lowering of the oxygen flow, the growth enters into zinc rich growth. There are many considerations when moving into this environment. Firstly, as the oxygen plasma flow is reduced, the oxidation rate at the substrate surface is reduced. This pushes the equilibrium dynamics at the substrate surface to a thermodynamically stable configuration, leading to lattice latching. Here the film will preferentially grow with the same lattice parameters as the substrate so as to minimize the biaxial compressive strain at the film [4]. This is accompanied by a redistribution of the Mg so as to minimize the discontinuity at the substrate-film interface.

The films with varying Mg concentration are nonetheless of interest in that they will have a varying band energy throughout the film, thereby reducing the degree to which carriers are confined. By diluting the charge carriers, the build up of non-equilibrium polar optical phonons will be reduced. This is a limiting factor to the velocity of the charge carriers in a high density 2DEG.

3.2.3 Film Growth Summary

The effects of changing three main growth variables have been demonstrated: Mg flux, O_2 flow and temperature. All three variables changed the composition and structure of the thin film significantly. Reducing the growth temperature from 750 °C to 500 °C caused the Mg concentration to reduce and the quality of the film to degrade as measured by XRD. Decreasing the oxygen flow moves the growth from the kinetically favourable route of constant concentration of Mg to the thermodynamically stable film growth resulting in a gradient of Mg throughout the film. Finally

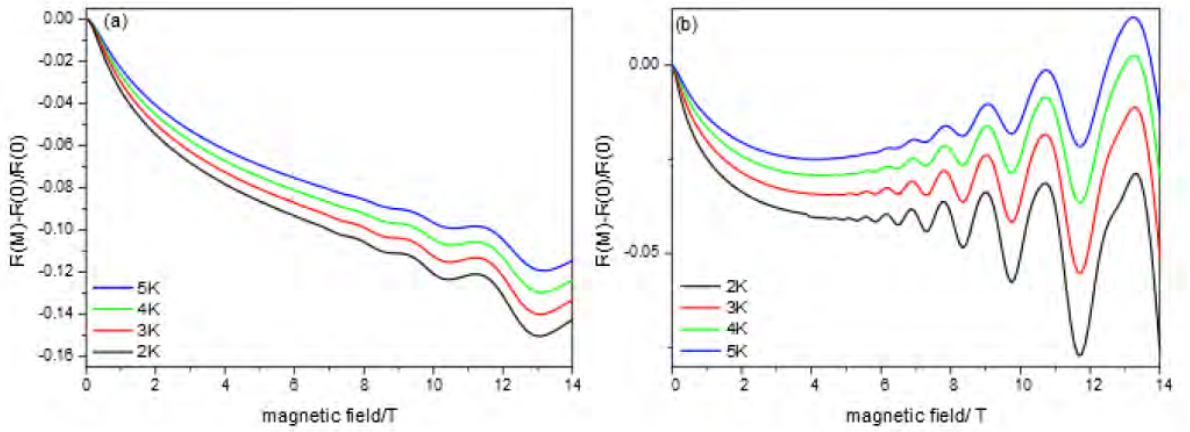

Figure 5: Longitudinal magnetoresistance of (a) sample A (grown at an oxygen flow rate of 2 sccm) and sample D (grown at an oxygen flow rate of 1 sccm) showing Shubnikov de Haas oscillations at high magnetic field and low temperature. The field is applied perpendicular to the interface.

reducing the Mg flux initially inhibits the formation of MgO, creating a homogeneous film, but then eventually results solely in surface Mg incorporation, a problem that has yet to be solved.

With these films a basic understanding of the interface dynamics can be ascertained. Ideally the next growths will take the growth conditions of the films discussed in this section, but be grown on a ZnO buffer layer deposited in situ. This has been shown to increase the mobility of the 2DEG, indicating that a more confined 2DEG has been created

3.3 Electrical Transport Characteristics of ZnO/ZnMgO Interfaces

3.3.1 Introduction

The electrical transport properties of the thin films discussed above have been investigated. For the magnetic field dependence, the samples were measured between 0.4 K and 2 K. By applying a magnetic field perpendicular to the current direction, the Landau levels are shifted relative to the Fermi energy and become more separated in energy allowing the quantization of the levels to be observed. With transitions between other states forbidden by the Pauli exclusion principle, in principle a zero resistance state can be observed in the longitudinal direction. By observing Shubnikov de Haas (SdH) oscillations many parameters of the 2DEG system can be calculated, such as the sheet charge carrier concentration, the mobility, the effective mass and the quantum scattering rate.

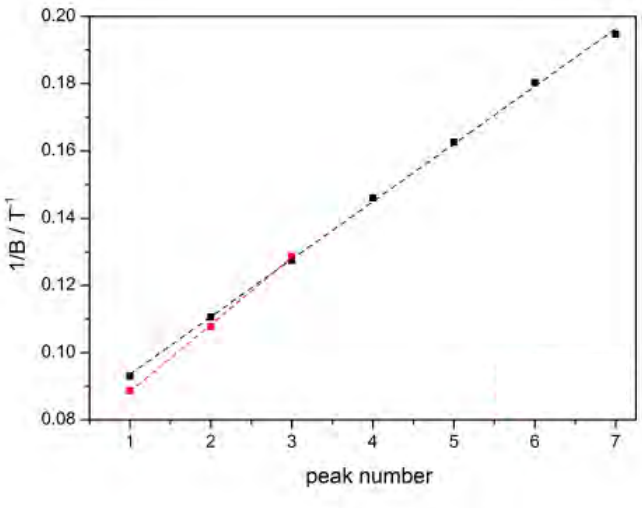

Figure 6: Inverse magnetic field at which each MR peak in figure 5 occurs at T = 2 K, plotted as a function of (arbitrary) peak number index. Red: sample A; black: sample D. The lines show linear fits from which the carrier concentration is extracted.

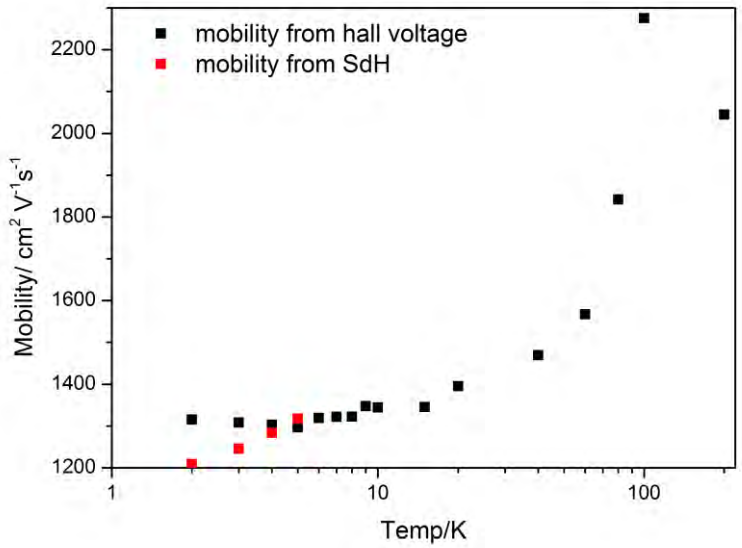

Figure 7: Temperature dependence of the mobility of sample A, determined by Hall measurements (black points) and SdH oscillations (red points)

3.3.2 Type I Films

As previously discussed, to form a true 2DEG there needs to be an abrupt interface. With this in mind, the samples with approximately constant Mg content throughout the film (*i.e.* those grown at an oxygen flow rate of 3 sccm) were initially investigated. On applying a 14T magnetic field, none of these Type I samples exhibited any SdH oscillations. Even with good film quality, determined by the XRD and XPS measurements, the interface quality was not good enough to see confinement of the electrons. This could be due to sample preparation or due to substrate quality. A range of different substrate preparation techniques are now being investigated, as well as more investigation into the initial ZnO buffer layer growth.

3.3.3 Type II Films

As shown in figure 4, for films grown at an oxygen flow rate of 2 sccm or lower the Mg redistributes itself away from the ZnMgO/ZnO interface, leading to what we call a Type II film. Both of these films exhibit Shubnikov de Haas (SdH) oscillations, indicative of quantum transport via edge states in a two-dimensional electron gas. These oscillations are shown in figure 5. Figure 6 shows a plot of the inverse of the field at which the local resistance maxima occur as a function of an arbitrarily assigned peak number index, the linearity of which confirms the quantum nature of the resistance oscillations in figure 5. Furthermore from the gradient of figure 6 we extract a carrier concentration of $2.9 \times 10^{12} cm^{-2}$ at 2K for sample D and $2.2 \times 10^{12} cm^{-2}$ at 2K for sample A. These carrier concentrations were independently confirmed by measurements of the Hall effect in the same samples.

The values of mobility extracted from the SdH oscillations are 1300 $cm^2V^{-1}s^{-1}$ and 1500 $cm^2V^{-1}s^{-1}$ for sample A and D respectively. This can be compared with the mobility of undoped ZnO, which is reported to be 12 $cm^2V^{-1}s^{-1}$ at 2K [5]. The temperature dependence of the mobility of sample A is shown in figure 7. At low temperatures the Hall mobility is found to be temperature independent. A maximum mobility of 2200 $cm^2V^{-1}s^{-1}$ is found at 100 K.

The effective mass m^* is in the range $0.30m_e$ to $0.42m_e$ for sample D and 0.40 m_e to $0.55m_e$ for sample A. The large range of spread within the effective mass is due to there still being a conduction path parallel to the confined electrons. This conduction path is the cause of the non-zero resistance of the SdH troughs and the large variation in resistance at low magnetic field.

4 Conclusions

We used molecular beam epitaxy to grow ZnMgO/ZnO interfaces with electron mobilities as high as 2200 $cm^2V^{-1}s^{-1}$. This enabled us to measure quantum oscillations in the resistance of the interfaces as shown in figure 5. In our experiments the highest mobilities were obtained for ZnMgO films in which the Mg concentration is spatially varying through the thickness of the film. This Mg redistribution occurs during film growth and has the effect of minimising the strain at the ZnMgO/ZnO interface. It is likely therefore that the mobility of films showing a uniform Mg distribution is limited by this interfacial strain. Ongoing work therefore will focus on tailoring the properties of the interface during growth so as to simultaneously maximise the electron confinement and minimise the strain. This will necessitate the growth of a thin film of ZnO between the ZnO single crystal substrate and the ZnMgO thin film.

References

[1] W. I. Park *et al. Appl. Phys. Lett.* **79** 2022 (2001)

[2] M. J. Manfra *et al. Appl. Phys. Lett.* **85** 1722 (2004)

[3] H. Morkoç and Ü. Özgür, *Zinc Oxide: Fundamentals, Materials and Device Technology* (Wiley, 2008)

[4] J. Ye *et al. Sci. Rep.* **2** 533 (2012)

[5] M. Sundaram *et al. J. Appl. Phys.* **76** 1003 (1994)

List of Symbols, Abbreviations and Acronyms

2DEG	two-dimensional electron gas
AFM	atomic force microscope
DOD	Department of Defense
FRAM	ferromagnetic random access memory
IPA	isopropyl alcohol
MBE	molecular beam epitaxy
m_e	electron mass
PPMS	Physical Properties Measurement System
RHEED	reflection high energy electron diffraction
rpm	revolutions per minute
sccm	standard cubic centimetres per minute
SdH	Shubnikov de Haas
T	Tesla
THz	terahertz
V_{bb}	band-bending potential
XPS	x-ray photoelectron spectroscopy
XRD	x-ray diffraction
θ	angle of x-ray incidence